The Journal of Chemical Physics ARTICLE scitation.org/journal/jcp

Modeling the α- and β-resorcinol phase boundary via combination of density functional theory and density functional tight-binding

Cite as: J. Chem. Phys. 154, 134109 (2021); doi: 10.1063/5.0044385
Submitted: 15 January 2021 • Accepted: 10 March 2021 •
Published Online: 2 April 2021

Cameron Cook, Jessica L. McKinley, and Gregory J. O. Beran[a)]

AFFILIATIONS

Department of Chemistry, University of California, Riverside, California 92521, USA

Note: This paper is part of the JCP Special Topic on Computational Materials Discovery.
[a)]**Author to whom correspondence should be addressed:** gregory.beran@ucr.edu. **Telephone:** +1 951 827-7869

ABSTRACT

The ability to predict not only what organic crystal structures might occur but also the thermodynamic conditions under which they are the most stable would be extremely useful for discovering and designing new organic materials. The present study takes a step in that direction by predicting the temperature- and pressure-dependent phase boundary between the α and β polymorphs of resorcinol using density functional theory (DFT) and the quasi-harmonic approximation. To circumvent the major computational bottleneck associated with computing a well-converged phonon density of states via the supercell approach, a recently developed approximation is employed, which combines a supercell phonon density of states from dispersion-corrected third-order density functional tight binding [DFTB3-D3(BJ)] with frequency corrections derived from a smaller B86bPBE-XDM functional DFT phonon calculation on the crystallographic unit cell. This mixed DFT/DFTB quasi-harmonic approach predicts the lattice constants and unit cell volumes to within 1%–2% at lower pressures. It predicts the thermodynamic phase boundary in almost perfect agreement with the experiment, although this excellent agreement does reflect fortuitous cancellation of errors between the enthalpy and entropy of transition.

I. INTRODUCTION

Organic molecular crystal structure prediction (CSP) has progressed dramatically in recent years, including many successful "blind" predictions.[1–8] CSP is increasingly being employed to understand pharmaceutical solid form landscapes,[9–17] for example. While polymorph stability rankings of experimentally known structures are often predicted with reasonable accuracy, one of the long-standing challenges of CSP lies in understanding why crystal energy landscapes frequently include far more putative structures than have been observed experimentally.[18] In some cases, McCrone's remark[19] that the number of crystal structures known for a compound is proportional to the time and money spent searching for them seems to hold true. Nevertheless, the number of predicted structures greatly exceeds the number of experimentally known ones even for prolific polymorph formers such as ROY (5-methyl-2-[(2-nitrophenyl)-amino]-3-thiophenecarbonitrile),[20,21] galunisertib,[15] and axitinib.[22]

One partial explanation for this failure to observe predicted polymorphs lies in the idea that researchers simply have not yet provided the correct crystallization conditions for these forms. Kinetics plays an important role in the phenomenon of polymorphism, as exemplified by the recent reports of two new ROY polymorphs, which were discovered via non-traditional crystallization techniques.[23,24] Unfavorable kinetics has also been invoked to explain why the predicted "global minimum" polymorph of galunisertib has not been found experimentally despite years of effort,[15] although recent work has also argued that the high stability of that polymorph may be an artifact of density functional theory (DFT).[25]

In 2018, Price described current-generation crystal structure prediction approaches that search for the global lattice energy minimum structure as "zeroth-order" CSP.[26] The next generation "thermodynamic" CSP would rank structures based on the free energy as a function of temperature and pressure, as well as on the crystal size, solvent, and the presence of heterogeneous templates or

impurities. The free energy landscape can differ considerably from the lattice energy one due to factors such as the phonon contributions or dynamic behaviors that cause multiple lattice energy minima to coalesce[27–29] into a single free energy basin. Overall, thermodynamic CSP represents a greater challenge to computational chemistry: moving beyond predicting what polymorphs might form to predicting the experimental conditions under which they will be most likely to form. This has been realized already in select cases. For the drug candidate Dalcetrapib, for example, CSP prediction of a stable densely packed polymorph led to a subsequent successful high-pressure crystallization of that form.[12]

Aiming toward the goal of predicting polymorph stability as a function of temperature and pressure, the present work focuses on predicting the structures, thermochemical properties, and thermodynamic phase boundary between two polymorphs of resorcinol. Predicting phase transition temperatures is particularly difficult for several reasons. Beyond the fundamental challenge of predicting accurate lattice energies, one must also compute phonon contributions to the free energy. Vibrational contributions also typically induce thermal expansion of the crystal lattice, and accounting for how the resulting anharmonicities impact free energies [e.g., via the quasi-harmonic approximation (QHA)[30–32]] can be critical to predicting even qualitatively correct phase boundaries.[33] Further treatments of anharmonicity and/or quantum effects can also be considered.[27,34–44] Uncertainty analysis indicates how the predicted thermal phase transition temperatures can exhibit strong sensitivity to small errors.[45] In particular, the more parallel the free energy curves are for different phases, the greater the impact of small errors on the predicted phase boundary. High-pressure phase boundaries can be moderately easier to predict, since thermal expansion is reduced and packing density becomes a major factor in determining the enthalpy at high pressures.

Despite these challenges, there have been a number of successful predictions of phase boundaries in systems such as carbon dioxide,[46–51] ice,[52,53] nitrogen,[54–59] methanol,[33] benzene,[27,34,39,60] and others.[35,61] In methanol, for example, fragment-based calculations at the coupled-cluster singles, doubles, and perturbative triples [CCSD(T)] level coupled with the quasi-harmonic approximation predicted the phase diagram of the α, β, and γ to within ~0.5 kJ/mol accuracy over a range of several hundred Kelvins and a few GPa.[33]

Unfortunately, that coupled cluster theory prediction of the methanol phase diagram required a few hundred thousand central processing unit (CPU) hours[33] and applying the same techniques to pharmaceutical-sized molecules would be infeasible. Density functional theory is considerably less computationally demanding, although it can still be expensive due to the high cost of computing harmonic phonons with DFT. Instead, the current study utilizes a quasi-harmonic model that combines density functional theory (DFT) treatment of the lattice energies and a recently developed approach[62] for obtaining the phonon density of states (DOS) from a mixture of DFT and density functional tight binding (DFTB). In particular, the high computational cost of the phonon calculation is exacerbated by the need for large supercells to obtain well-converged phonon densities of states. The new approach first computes the phonon density of states in a large supercell with DFTB at a relatively low cost and then shifts the individual phonon bands based on the difference between DFT and DFTB frequencies in a smaller crystallographic unit cell. This ensures DFT-quality phonon modes at the Γ point, while the phonon dispersion is modeled with DFTB.

A number of earlier studies have found dispersion-corrected DFTB3 models to be useful in molecular crystal applications,[63–65] including for embedding models,[66] intermediate screening steps in crystal structure prediction,[67,68] and for quasi-harmonic calculations.[69] This evidence suggests that the same DFTB3 models may be suitable for the present phonon approximation as well. In testing on a few simple crystals using dispersion-corrected third-order DFTB3-D3(BJ) and the B86bPBE-XDM density functional,[62] the approximation introduced ~1 kJ/mol errors or less into the total Gibbs free energies compared to the DFT ones. Additional error cancellation occurred in the relative energy differences between different crystal polymorphs. At the same time, the mixed DFT/DFTB approach reduced the computational effort required for evaluating the phonon density of states by 1–2 orders of magnitude compared to a more conventional approach based purely on DFT.

The present study extends that earlier research by combining this phonon density of states approximation with the quasi-harmonic approximation and then modeling the crystal structures and phase transition of the α and β polymorphs of resorcinol at finite temperatures and pressures. Resorcinol, also known as benzene-1,3-diol, has been studied for many decades and is used in the synthesis of resins and pharmaceuticals. Crystalline resorcinol can occur in several known polymorph phases. The α and β phases adopt the same $Pna2_1$ space group, although they differ in their intramolecular conformations and intermolecular hydrogen bonding patterns (Fig. 1).[70]

The α polymorph is the thermodynamically preferred form under ambient conditions, even though it is less dense than the β phase (i.e., contrary to the density rule.[71]). The α phase converts to the β polymorph upon heating to ~360–370 K or at room temperature upon compression at ~0.4–0.5 GPa.[70,72,73] The transition temperature and pressure depend strongly on both the rate of heating and the rate of pressurization, implying that kinetics plays a role in the phase transition.[72,74–76] The experimental phase observations used here result from careful measurements, which attempted to control these kinetic factors through sample equilibration and by using slower heating and pressurization rates.[72,74]

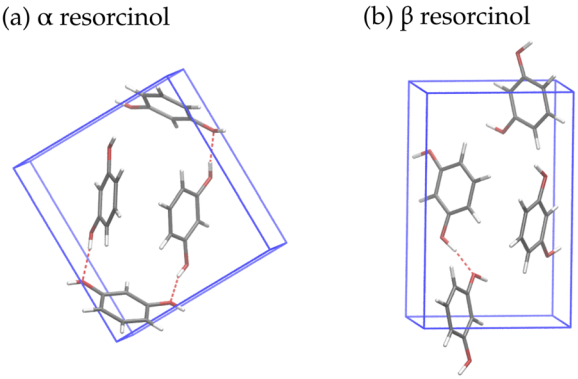

FIG. 1. The crystal structures of α and β resorcinol differ in the hydroxyl group orientations and their intermolecular hydrogen bond networks.

Three other phases of resorcinol are not considered here. The disordered γ polymorph and the ordered δ one form at several GPa of pressure, although neither crystal structure has been solved.[72,75,76] In 2016, the structure of a new ϵ polymorph was reported under atmospheric conditions through a combination of experimental powder x-ray diffraction and crystal structure prediction, and there was even some evidence of another (as yet unconfirmed) $P2_1$ phase.[77] However, this ϵ polymorph is believed to be metastable relative to the α and β phases at all temperatures, so it is not considered here either. Section II describes the approximation used for the phonon density of states and its incorporation into the quasi-harmonic approximation.

II. THEORY

A. Gibbs free energies

The thermodynamic stability of a crystal at a given temperature and pressure is governed by the Gibbs free energy,

$$G(T,P) = U_{el} + F_{vib}(T) + PV, \tag{1}$$

where U_{el} is the electronic energy, $F_{vib}(T)$ is the Helmholtz vibrational free energy, and PV represents the pressure–volume contribution. The electronic energies here will be computed with DFT using periodic boundary conditions. Within the harmonic approximation, the Helmholtz vibrational free energy is computed as

$$F_{vib}(T) = 3nN_a k_B T \int_0^\infty \ln\left[2\sinh\left(\frac{\hbar\omega}{2k_B T}\right)\right] g(\omega)\, d\omega, \tag{2}$$

where n is the number of atoms in the crystallographic unit cell, N_a is Avogadro's number, $\hbar$ is Planck's constant, k_b is the Boltzmann constant, T is the temperature, and $g(\omega)$ is the phonon DOSs as a function of frequency ω.[78]

B. Efficient approximation for the phonon density of states

Because evaluation of the harmonic phonon DOSs often forms the major computational bottleneck in computing the free energy, approximations that reduce the cost of the phonon DOS can be very helpful. One of the simpler phonon DOS approximations is to evaluate only the zone-center (Γ-point) phonons. However, this approximation neglects contributions arising from dispersion of the optical phonon modes throughout reciprocal space and the non-zero frequencies of the acoustic modes away from the Γ point. Acoustic modes contribute significantly to the entropy and to the temperature dependence of the enthalpy. They can be important when predicting thermodynamic phase boundaries, where even small errors in the free energy can shift the transition temperature by a hundred degrees Kelvin or more. These contributions away from the Γ point are generally expected to be most important in smaller unit cells for which the Γ-point phonon DOS is less-well converged and in cases where the unit cell shapes differ considerably between polymorphs, thereby hindering error cancellation in the thermochemical energy differences.

Phonon contributions away from the Γ point can be captured by performing a supercell lattice dynamics calculation[31,79,80] or using density functional perturbation theory.[81] Unfortunately, the need for large supercells extending ~10–15 Å or more in each direction to converge the phonon density of states[38,79,82] makes the supercell approach far more expensive than a simple harmonic phonon calculation on the crystallographic unit cell. To address this computational bottleneck, we recently proposed a strategy[62] for approximating the phonon density of states, which reduces the computational cost by ~1–2 orders of magnitude while introducing only small errors into the resulting free energies. This approach first performs the lattice dynamics calculation in a large supercell with density functional tight binding (DFTB) to capture the optical mode phonon dispersion. However, individual DFTB phonon bands will often be shifted considerably in frequency from the DFT values due to the limitations of the DFTB model, which leads to substantial errors in the resulting free energies. To improve the DFTB phonon DOSs, the harmonic phonons are computed at the Γ point using DFT. This DFT unit cell calculation is typically far less computationally demanding than a large DFT supercell calculation would be. Each DFTB normal mode is then assigned to the corresponding DFT mode based on the overlap of the normal mode eigenvectors, and an additive shift is applied to the frequencies of each DFTB phonon band based on the difference between the DFT and DFTB frequencies at the Γ point. The normal mode matching is similar to how eigenvector overlaps can be used to identify common normal modes in a crystal structure at multiple different volumes, for example.[83] Previous testing in other crystals[62] and for resorcinol here suggests that the mode assignments based on maximal overlaps are generally straightforward. After reordering the phonon modes based on the matched pairs, the overlap matrix becomes highly diagonally dominant, and virtually all the diagonal overlap elements between the DFT and DFTB normal mode eigenvectors exceed 0.5 (also they are often closer to unity).

This phonon mode matching procedure ensures that the Γ-point phonon values match DFT, while the phonon dispersion away from the Γ point is modeled by DFTB. Because this shift is not applicable to the three acoustic modes (their frequencies are always zero at the Γ point), the acoustic mode frequencies are computed from DFT elastic constants using the theory of elasticity.[84] Finally, the phonon density of states is constructed using a kernel density estimation (KDE) in which a 5 cm^{-1} wide normal distribution is placed at the frequencies from each discretely sampled k-point. This KDE approach improves the convergence of thermal properties with respect to reciprocal space sampling.[84] In small-molecule crystal benchmarks, this phonon DOS approximation approach introduced errors of ~1 kJ/mol or less into the total free energies compared to supercell DFT results. Further error cancellation appears to occur for the relative free energies between crystal forms (see Ref. 62 for further details).

To help visualize this approximation, Fig. 2 plots a sample phonon DOS for α-resorcinol before and after applying the frequency shift. These phonon densities of states use the DFTB3-D3(BJ) model and the generalized gradient approximation (GGA) functional B86bPBE-XDM that will be described in Sec. III. As seen here, the correction shifts the phonon modes considerably. The most substantial changes occur in the intramolecular stretching region above ~1000 cm^{-1}. Some of the C–H stretching modes shift by hundreds of cm^{-1}. However, there are also many less visible changes in the density distribution in the lower-frequency region. Over-

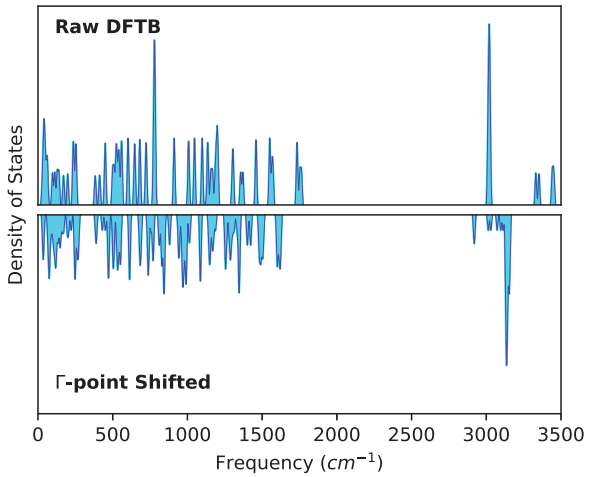

FIG. 2. Comparison of the DFTB3-D3(BJ) phonon density of states for α resorcinol before and after applying the B86bPBE-XDM DFT Γ-point frequency shift.

all, the average magnitude of the frequency shift is 78 cm^{-1}, and these changes impact the thermochemistry considerably. The zero-point enthalpy increases by 2.4 kJ/mol per molecule, although the shift in the thermal enthalpic contributions exhibits the opposite sign, and the total enthalpy shift at 300 K is only 0.9 kJ/mol. The impact on the entropies is even larger. The frequency shift reduces the entropy by 17.1 J/(mol K) at room temperature, which reduces the entropic contribution TS to the free energy by 5.1 kJ/mol. The final free energy is shifted by 6.1 kJ/mol. Similar magnitude shifts occur for the β polymorph as well, leading to partial cancellation of these corrections in the relative polymorph energy difference. Nevertheless, these results highlight the significant impact of applying the Γ-point shift to the DFTB phonons. Finally, we note that this phonon DOS approximation is not restricted to particular DFTB or GGA functional models used here; any combination of a computationally inexpensive model with a more expensive higher-accuracy model could be used. As will be demonstrated in Sec. IV, the chosen combination works fairly well for resorcinol, but it is possible that the results could be improved further with alternative model choices.

C. Quasi-harmonic approximation

Anharmonic contributions can also contribute appreciably to the predicted thermochemical energies. The QHA represents one of the simplest approaches for incorporating some anharmonicity into the harmonic phonon treatment. It typically works fairly well for molecular crystals up to moderately high temperatures below the melting point.[30,31] The QHA maps how the phonon frequencies and free energies vary with the molar volume of the crystal. In the implementation here, the electronic energy U_{el} is first computed as a function of volume by applying a series of positive and negative external isotropic pressures to the cell and relaxing the lattice parameters and atomic positions. This allows the unit cell to relax anisotropically, softens the one-dimensional potential energy curve compared to isotropic scaling of the lattice constants, and leads to improved description of the expansion/contraction.[33,85]

Next, the phonon density of states and free energies are evaluated at the equilibrium geometry and at several expanded and contracted volumes from the $U_{el}(V)$ curve. Each explicit phonon DOS evaluation was performed using the mixed DFT/DFTB approach described in Sec. II B, and care was taken to ensure that the phonon DOS calculations were performed across the range of volumes associated with the temperatures and pressures of interest. After computing $F_{vib}(T)$ for each sampled structure at a chosen temperature, the F_{vib} values as a function of volume were fitted to a second-order polynomial. This F_{vib} fitting procedure appears to work well [see Fig. 3(b) and Refs. 33 and 86–88], although one could alternatively fit the individual phonon frequencies as a function of volume.[69] Summing $U_{el}(V)$, $F_{vib}(V)$, and PV for the given temperature and pressure produces $G(V)$. This free energy is fitted to a double-Murnaghan equation of state in which the compression and expansion branches are fitted separately to the Murnaghan equation of state,[89]

$$G(V) = G_0 + \frac{B_0 V}{B_0'}\left[\frac{(V_0/V)^{B_0'}}{B_0' - 1} + 1\right] - \frac{B_0 V_0}{B_0' - 1}, \tag{3}$$

and the two halves connect smoothly at the equilibrium volume V_0. From the fit, one obtains the optimal molar volume V_0, free energy at that volume G_0, the bulk modulus B_0, and the first derivative of the bulk modulus with respect to pressure, B_0'. The double-Murnaghan form was chosen based on a prior study of crystalline methanol, which found the *ab initio* free energy data reproduced more accurately than several other common functional forms.[85] Figure 3 plots sample the electronic energy, Helmholtz vibrational free energy, and combined Gibbs free energies vs volume for the two resorcinol polymorphs at room temperature and ambient pressure.

The computational bottleneck lies in computing the electronic energy curve and phonons. The subsequent steps described here to determine the optimal structure at a particular temperature and pressure require minimal computational cost, which allows one to map out $G(T, P)$ readily. Lattice parameters and atomic coordinates for the current volume are interpolated from the values explicitly obtained in the geometry optimizations used to generate $U_{el}(V)$.

The specific form of the quasi-harmonic approximation used here does make some approximations. The thermal expansion is mapped onto a one-dimensional quasi-anisotropic dependence on the volume. Moreover, the atomic positions at each given volume/pressure are optimized based on the electronic lattice energy, rather than the free energy. As a result, contributions from zero-point vibrational energy and the anisotropy of the thermal expansion are only partially captured. Nevertheless, approaches similar to the one used here have proved successful in many applications.[8,31–33,38,83,85–88,90–92] Moreover, Abraham and Shirts studied different quasi-harmonic approximations for predicting thermal expansion and polymorph free energies in organic molecular crystals, including for the α and β polymorphs of resorcinol. At room temperature, they found that an approach similar to the one used here differed from more complete quasi-harmonic approximation models by no more than 0.5% in lattice parameters and ~0.1 kJ/mol in the free energy difference between the two polymorphs. That will not always be true: they found less faithful performance for

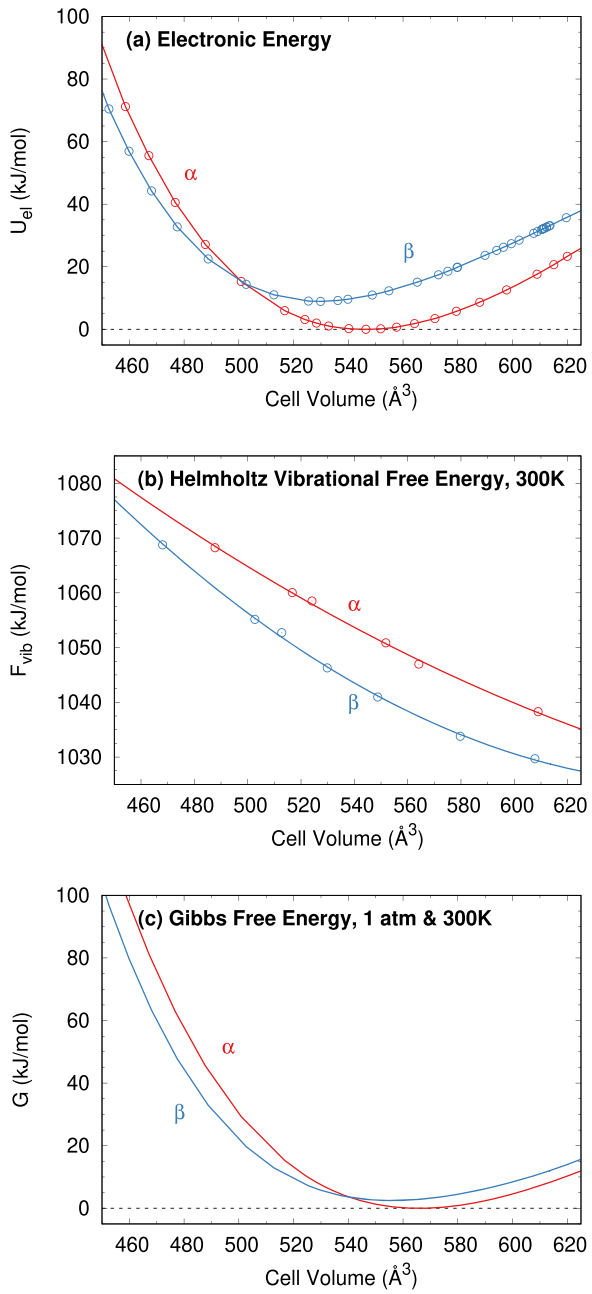

FIG. 3. The quasi-harmonic treatment of resorcinol combines (a) electronic DFT energies and (b) Helmholtz vibrational free energies as a function of volume, which are then summed along with the *PV* term to obtain (c) the Gibbs free energy. The predicted structures for the given thermodynamic conditions correspond to the minima of the *G*(*V*) curves. Data shown here for 300 K and 1 atm.

an approximation like the one used here when studying two polymorphs of piracetam, however, and further work is needed to ascertain more clearly when more elaborate treatments such as those found in Refs. 36 and 93 will be required.

III. COMPUTATIONAL METHODS

A. DFT structure optimizations

Experimental crystal structures for α- (RESORA03[94]) and β-resorcinol (RESORA08[95]) under ambient pressure were taken from the Cambridge Structure Database (CSD). The experimental α structure was solved at 120 K, while the β-form one was determined at room temperature. The atomic positions and lattice parameters for each structure were fully relaxed to their electronic energy minima using plane wave DFT. The electronic energy surface U_{el} was mapped out over 37 volumes spanning 408–720 Å^3 for α and 39 volumes spanning 408–638 Å^3 for β through a series of additional structure relaxations subjected to positive and negative external isotropic pressures. Similar equation of state fits could likely have been obtained with fewer energy-volume data points as well.

These periodic DFT calculations were performed in Quantum Espresso v6.1[96] using the B86bPBE density functional[97,98] and the exchange-hole dipole method (XDM) dispersion correction.[99] This functional has performed well in many earlier molecular crystal studies.[6,7,99,100] Core electrons were treated according to the projector augmented wave (PAW) approach, and PAW potentials for H, C, and O were produced using A. Dal Corso's Atomic code v6.1.[101] Optimizations were carried out using a 50 Ry plane wave energy cutoff. Reciprocal space k-points were placed on a 1 × 1 × 3 Monkhorst–Pack grid[102] for α-resorcinol and on a 3 × 1 × 3 grid for β-resorcinol.

B. Phonon density of states and free energies

DFT and DFTB3-D3(BJ) harmonic vibrational frequencies were computed using the finite displacement method, as implemented in Phonopy v2.4.2.[80] DFT Γ point phonons were evaluated using the same B86bPBE-XDM density functional, k-point grid, and plane wave cutoff, as described in the optimization procedure.

To ensure stationarity of the DFTB potential energy, the atomic positions in the unit cells were subsequently optimized with DFTB3-D3(BJ) prior to supercell expansion using the DFTB+ software, version 19.1.[103,104] The DFTB3-D3(BJ) calculations employed the 3ob-3-1 Slater–Koster parameterization,[105] which has shown good performance for organic species,[106] and Grimme's D3 dispersion correction.[107] All other DFTB job parameters employ the default values recommended in the DFTB+ documentation. The optimized DFTB structures were expanded to 3 × 3 × 4 supercells for both structures. For the equilibrium structures, this corresponds to a minimum supercell dimension of 31 Å × 28 Å × 22 Å for α and 23 Å × 38 Å × 21 Å for β, each consisting of 2016 atoms. Similar results could probably been obtained with smaller supercells, but these large cells were chosen to ensure good convergence of the phonon DOS, and they were affordable with DFTB3-D3(BJ). Finally, the Helmholtz vibrational free energies were computed from the phonon DOS via numerical integration of Eq. (2). The quasi-harmonic approximation calculations and phase-diagram predictions were managed via an in-house python script, which is available on GitHub at https://github.com/cjcook41/Modematching. Inelastic neutron scattering (INS) spectra were simulated using the OCLIMAX program, version 3.0.[117,126]

For perspective on the computational timings, optimizing the α polymorph geometry from the experimental structure required

90 central processing unit (CPU) core hours on an Intel Xeon E5-2680v3 processor. Computing the Γ-point phonons and the elastic constants for a single structure (56-atom unit cell) required 139 and 446 CPU core hours, respectively. Finally, the DFTB phonon frequency calculation on the 2016-atom supercell required 8260 core hours.

IV. RESULTS AND DISCUSSION

A. Assessment of thermal expansion

First, we investigate the quality of the predicted unit cell volumes for both polymorphs relative to the experiment under ambient pressure. Table I shows the predicted and experimental lattice parameters and unit cell volumes at select temperatures for α- and β-resorcinol. The optimized B86bPBE-XDM lattice parameters obtained from pure lattice energy minimization (i.e., without employing the quasi-harmonic approximation) are also included for comparison with the QHA results.

The QHA thermal expansion of the unit cell proves to be key to the accurate prediction of the experimental lattice parameters at all temperatures considered. Predicted cell volumes and lattice parameters for α-resorcinol are in excellent agreement with the experiment.[94] Inclusion of the zero-point vibrational contribution and heating to 120 K causes a 2.7% volume expansion in α resorcinol. At 120 K, the QHA cell volume is only 0.7% smaller than the experimental volume, whereas the purely electronic DFT structure without QHA phonon contributions underestimates the volume by 3.2%. The 120 K QHA lattice constants also exhibit excellent agreement with those determined experimentally, with errors of 0.02 Å or less.

In β-resorcinol, even at extremely low temperatures (4 K), QHA expansion leads to a 3.2% increase in volume with respect to the electronic minimum. This expansion again improves agreement with the experimental volume at 4 K, reducing the error from 2.6% too small without the QHA to only 0.5% too large with the QHA. This low temperature expansion primarily originates from the zero-point vibrational energy contributions, as the thermal population of the density of states is quite low. At room temperature, further expansion in the experimental cell means that the electronic energy minimum (no QHA) structures are 5.5% too small in volume, while the QHA treatment overestimates the volume by only 0.8%. In other words, the QHA treatment mildly exaggerates the expansion that occurs over the 0–300 K temperature range in this system.

The errors in the individual lattice parameters are somewhat larger for β-resorcinol than they were for the α polymorph, although they still exhibit reasonable agreement with the experiment. The *a* and *c* lattice constants are over-estimated by 0.07 Å and 0.03–0.06 Å, respectively, while *b* is underpredicted by 0.13–0.14 Å. The opposing signs of these errors lead to some error cancellation that leads to the excellent predicted cell volumes. The QHA model does correctly predict the slight contraction of the *b* lattice constant with the increase in the temperature seen in the experiments. This contraction of *b* coupled with expansion of *a* and *c* also highlights the importance of allowing anisotropic relaxation of the cell, constructing the initial $E(V)$ curves used in the QHA.[108]

Second, Fig. 4 compares the predicted thermal expansion of both polymorphs relative to experiment at 0.09 GPa.[72] The quasi-harmonic B86bPBE-XDM calculations underestimate the unit cell volume of α-resorcinol by about 1.5%–2% throughout the temperature range shown, while the β form volumes are overestimated by 1.2% on average. These errors are reasonably consistent with the results in Table I, especially when considering that the α polymorph results are above room temperature here, compared to 120 K in Table I. This level of agreement between theory and experiment is also consistent with the errors found for quasi-harmonic modeling in previous studies.[8,32,85,90,92,108–112] The quasi-harmonic model also reproduces the slope of the volume expansion with the temperature for both polymorphs fairly well in this temperature range. The opposite signs of the errors between the two phases do mean that the

TABLE I. Comparison of the predicted and experimental lattice parameters for the α and β polymorphs of resorcinol. The quasi-harmonic approximation is employed for the finite-temperature predictions, while the "no QHA" results utilize lattice energy minimization without any phonon contributions.

	Temperature	*a* (Å)	*b* (Å)	*c* (Å)	Cell volume (Å^3)
		α-resorcinol			
B86bBPBE-XDM	No QHA	10.37	9.32	5.58	539.91
B86bBPBE-XDM	120 K	10.45	9.40	5.65	554.27
Expt.[94]	120 K	10.47	9.41	5.67	557.95
		β-resorcinol			
B86bBPBE-XDM	No QHA	7.77	12.51	5.35	520.82
B86bBPBE-XDM	4 K	7.88	12.49	5.46	537.52
Expt.[95]	4 K	7.81	12.62	5.43	534.69
B86bBPBE-XDM	300 K	8.00	12.47	5.58	556.55
Expt.[95]	300 K	7.93	12.61	5.51	551.19

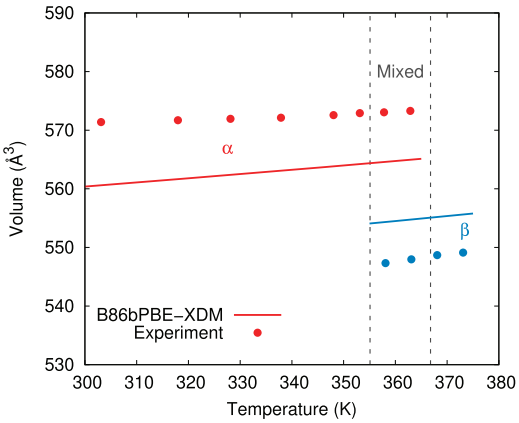

FIG. 4. Comparison of the experimentally reported unit cell volumes (points) for α- (red) and β-resorcinol (blue) at 0.09 GPA against those predicted from the quasi-harmonic B86bPBE-XDM calculations (lines). The vertical lines indicate the temperature regimes under which pure α, pure β, or a mixture of the two phases was observed experimentally.

predicted volume difference between the two phases is only about half the experimental difference, however.

Next, we investigate the quality of the predicted room-temperature unit cells as a function of pressure. Figure 5 compares the predicted volumes for both polymorphs from 0 to 4 GPa against experimental data from Refs. 72 and 70. The reported volumes from the two experimental studies are generally in good agreement. The plot also includes data from previous PBE-TS calculations from Ref. 73, which did not employ the quasi-harmonic approximation. For that reason, Fig. 5 shows B86bPBE-XDM data with and without quasi-harmonic thermal expansion. Without thermal expansion, the PBE-TS and B86bPBE-XDM volumes are very similar at low pressure for both phases, although PBE-TS predicts volumes that are consistently ~5–10 Å^3 larger than the B86bPBE-XDM ones. Both underestimate the experimental unit cell volume considerably below 1 GPa.

Upon applying the quasi-harmonic approximation with B86bPBE-XDM, the predicted unit cell volume expands by ~3%–5% for α and ~3%–7% for β, leading to much improved agreement with the experiment at pressures in the ~0–1 GPa range. As usual, thermal expansion occurs to a greater extent at lower pressures. Interestingly, all three computational models predict the resorcinol crystals to be considerably less compressible at higher pressures than the experiments, which leads to the cell volumes being considerably too large by 4 GPa. The reasons behind this discrepancy are unclear, but the fact that it occurs for all three models suggests that it is not due either to the specific generalized gradient approximation (GGA) density functionals used or to the inclusion/exclusion of phonon contributions. Regardless, the accuracy of the predicted volumes below 1 GPa is promising for predicting the phase transition in that regime.

Good agreement between the QHA B86bPBE-XDM model and the experiment[70] is also seen in the pressure dependence of the lattice constants, as shown in Fig. 6. For the α polymorph, the largest mean absolute error of 1.1% occurs for b, while a and c exhibit errors of only 0.2% and 0.5%, respectively. For β-resorcinol, the mean absolute errors are moderately larger at 1.3% for a, 0.9% for b, and 0.6% for c, but these still represent overall good agreement with the experiment.

B. Phase diagram and thermochemical properties

Having seen that the model reproduces the experimental crystal structures well at lower pressures, we now investigate the thermodynamic phase-transition boundary in the 0–1 GPa regime. The experimentally observed phase behaviors depend on sample purity, heating or pressurization rate, and, in some cases, the thermal history of the sample.[72,76] Early studies at ambient pressure reported the $\alpha \rightarrow \beta$ phase transition to occur at 344 K[113] or 347 K.[114] Ebisuzaki *et al.*[74] reported the α to β phase transition at 369 ± 6 K, followed by melting of the β phase at 382.8 ± 0.1 K. They attributed their higher phase-transition temperature to improved sample purity. Kichanov *et al.*[72] similarly reported the ambient-pressure $\alpha \rightarrow \beta$ phase transition at 363 K by monitoring the proton spin–lattice relaxation time using free induction decay amplitudes. The phase transition temperature decreases with the increase in pressure, and by 0.4 GPa, it occurs at room temperature. Figure 7 plots the experimentally observed phase behavior from Ref. 72. Over much of the pressure region, the precise thermodynamic phase boundary is not clear. Rather, the authors observed a long-lived mixed-state that contained seeds of the β phase nucleating within the α polymorph. The same mixed phase was also seen in earlier Raman studies.[76]

Figure 7 overlays the predicted quasi-harmonic B86bPBE-XDM thermodynamic phase boundary between the α and β phases on top of the experimental one. At ambient pressure, the phase transition is predicted to occur at 368 K, in nearly perfect agreement with the more recent experimentally reported transition temperatures of 363 K and 369 ± 6 K. At 0.4 GPa, the transition is predicted to occur at 260 K, in reasonable agreement with the experimental observation of a room-temperature transition at that pressure. The predicted slope of the phase-transition boundary with temperature

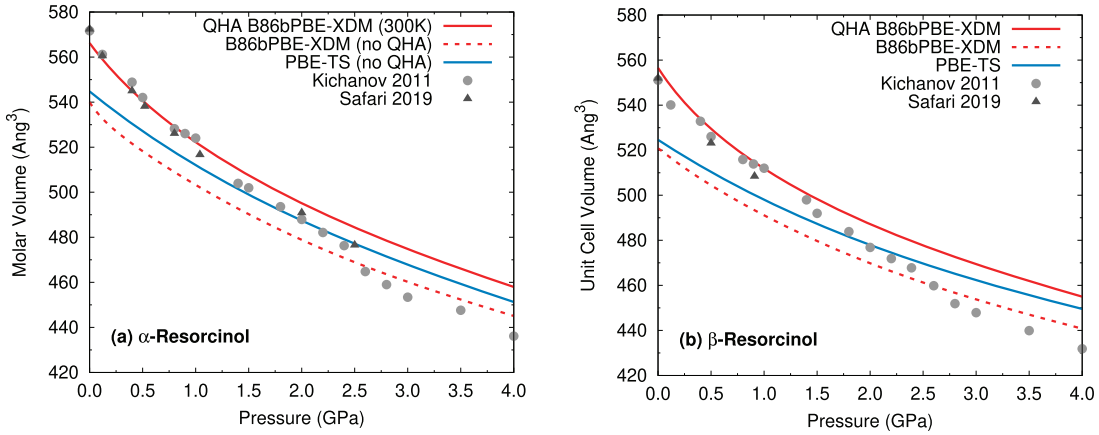

FIG. 5. Comparison of the predicted (lines) and experimental (points)[70,72] volumes of (a) α and (b) β resorcinol as a function of pressure. The quasi-harmonic approximation (QHA) B86bPBE-XDM predictions at room-temperature is in best agreement with the experiment at a low pressure, while the B86bPBE-XDM and PBE-TS[73] models without quasi-harmonic thermal expansion underestimate the volume at low pressures. All models overestimate the volumes to some extent at higher pressures.

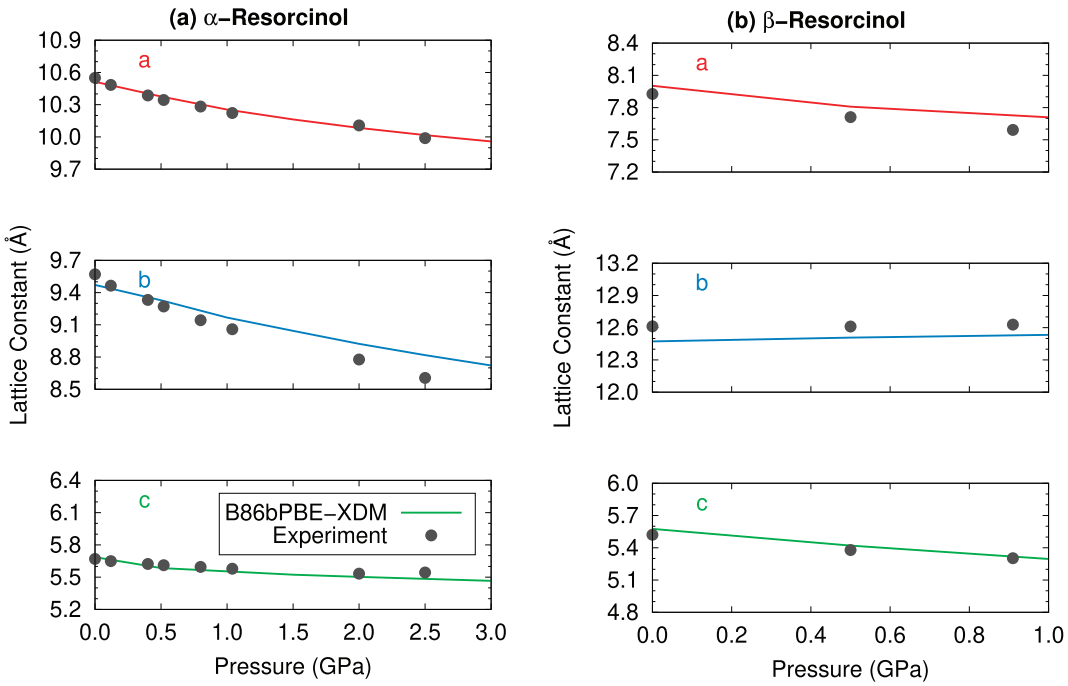

FIG. 6. Comparison of room-temperature experimental (points)[70] and predicted (lines) quasi-harmonic B86bPBE-XDM lattice parameters of (a) α and (b) β resorcinol as a function of pressure. (a) shows lattice parameters *a*, *b*, and *c* for the α polymorph, while (b) shows them for the β form.

and pressure appears qualitatively consistent with the experimental observations.

For further insight, sensitivity analysis is performed on the phase boundary by artificially stabilizing or destabilizing the α phase relative to the β one by up to 0.5 kJ/mol. The resulting phase boundaries are also plotted in Fig. 7. Shifting the polymorph free energy difference by ±0.5 kJ/mol causes the predicted transition temperature at zero-pressure to vary by ±80 K or roughly from ~290–450 K. The same shift alters the pressure-induced phase transition by ±0.3–0.4 GPa at room temperature. In other words, the predicted phase boundary is very sensitive to small errors in the Gibbs free energy, as has been noted previously for other systems.[33,45] In this light, the excellent agreement between theory and experiment here reflects a combination of good model accuracy and fortuitous error cancellation.

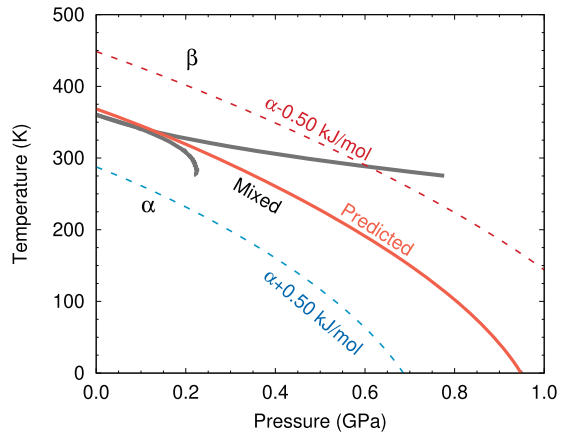

FIG. 7. Comparison of the experimentally observed[72] and predicted phase transition between α- and β-resorcinol. The red solid line corresponds to the predicted quasi-harmonic B86bPBE-XDM result, while the dotted lines indicate how the boundary changes if the α polymorph is artificially stabilized or destabilized relative to the β one.

To analyze the thermodynamic behavior more closely, Table II decomposes the free energy of transition at the phase transition temperature into its enthalpy and entropy components. Compared to the experiments of Ebisuzaki *et al.*[74] and by Bret-Dibat *et al.*,[115] the predicted $\Delta H_{\alpha\to\beta}$ is overestimated by 1–1.2 kJ/mol, reflecting a spurious stabilization of the α phase relative to the β one. The enthalpy error is largely compensated by a 2.6–3.0 J/mol K overestimation of $\Delta S_{\alpha\to\beta}$, which overstabilizes the β form relative to α at finite temperatures. Cancellation between these two errors produces the Gibbs free energy difference that leads to near perfect agreement in the predicted phase boundary.

The error in $\Delta H_{\alpha\to\beta}$ arises from a combination of the electronic lattice energy and phonon contributions, while the $\Delta S_{\alpha\to\beta}$ error stems primarily from the phonon contributions. As a crude numerical experiment, we examined how these two thermochemical quantities change when we shift the entire β-resorcinol phonon DOS toward higher frequencies. A +25 cm^{-1} phonon DOS shift decreases $\Delta H_{\alpha\to\beta}$ by about 0.25 kJ/mol, and a 50 cm^{-1} shift decreases $\Delta H_{\alpha\to\beta}$

TABLE II. Comparison of the predicted and experimental thermochemical data for the α to β phase transition of resorcinol under ambient pressure and the predicted/observed phase transition temperature.

Method	Source	$\Delta H_{\alpha\to\beta}$ (kJ/mol)	$\Delta S_{\alpha\to\beta}$ [J/(mol K)]	Temperature (K)
Expt.	Ebisuzaki *et al.*[74]	1.370 ± 0.007	3.71 ± 0.05	369 ± 6
Expt.	Bret-Dibat *et al.*[115]	1.2 ± 0.1	3.3	367 ± 0.4
B86bPBE-XDM	This work	2.33	6.26	368
B86bPBE-XDM Γ-point only	This work	2.17	5.97	364
PBE-TS, no QHA	Druzbicki *et al.*[73]	0.97	4.16	373[a]

[a] $\Delta H_{\alpha\to\beta}$ and $\Delta S_{\alpha\to\beta}$ were computed at 373 K, independent of the predicted phase-transition temperature.

by only 0.4 kJ/mol. In other words, only a fraction of the enthalpy error vs experiment likely stems from the phonon contribution; DFT errors in the lattice energy components are probably responsible for the larger fraction of the $\Delta H_{\alpha\to\beta}$ error. On the other hand, a ~25 cm^{-1} shift would be sufficient to bring $\Delta S_{\alpha\to\beta}$ into excellent agreement with the experiment. While the true phonon errors are surely more nuanced than a simple shift of the entire phonon DOS employed here, these results do suggest that the discrepancies between the predicted and observed thermochemical quantities in Table II can readily be accounted for within the expected errors of DFT.

Druzbicki *et al.*[73] computed $\Delta H_{\alpha\to\beta}$ and $\Delta S_{\alpha\to\beta}$ at 373 K using a variety of density functionals and the harmonic approximation. While most of the functionals they tested gave larger errors than those seen here, PBE-TS performed very well, with enthalpies and entropies of transition of 0.97 kJ/mol and 4.16 J/mol K at 373 K, despite neglecting thermal expansion. On the other hand, it appears that despite the better agreement between the enthalpy and entropy of transition, the error cancellation between the two is less effective: Although their study did not report the temperature dependence of $\Delta H_{\alpha\to\beta}$ and $\Delta S_{\alpha\to\beta}$, using the reported 373 K values would indicate a phase transition around 235 K, which is about 130 K below the experimental transition temperature. Furthermore, these PBE-TS thermochemical results were obtained for structures, which did not account for thermal expansion and therefore underestimate the molar volumes considerably (Fig. 5).

Next, in order to assess the impact of the phonon DOS approximation used here, we also examined the Gibbs free energies computed from the DFTB3-D3(BJ) phonon density of states (without applying the DFT Γ-point shift or acoustic mode correction). In that case, the two phases are incorrectly predicted to be monotropically related—i.e., α-resorcinol is thermodynamically preferred at all temperatures and pressures, and there is no $\alpha \to \beta$ phase transition. As shown in Figs. 8(a) and 8(c), enthalpy favors the α form throughout this temperature range for both phonon models, and the difference in $\Delta H_{\alpha\to\beta}$ between the two models is less than 0.8 kJ/mol. However, the two models predict completely different relative entropies. The polymorph entropy difference computed from the raw DFTB3-D3(BJ) phonon DOS has the wrong sign—it predicts that the α phase entropy is always greater than the β phase entropy (or in Fig. 8 that $-T\Delta S_{\alpha\to\beta}$ is positive). This error prevents the relative Gibbs free energy in Fig. 8(a) from changing sign. After applying both the DFT-based Γ-point shift and acoustic mode corrections, however, we see that the relative entropy reverses sign

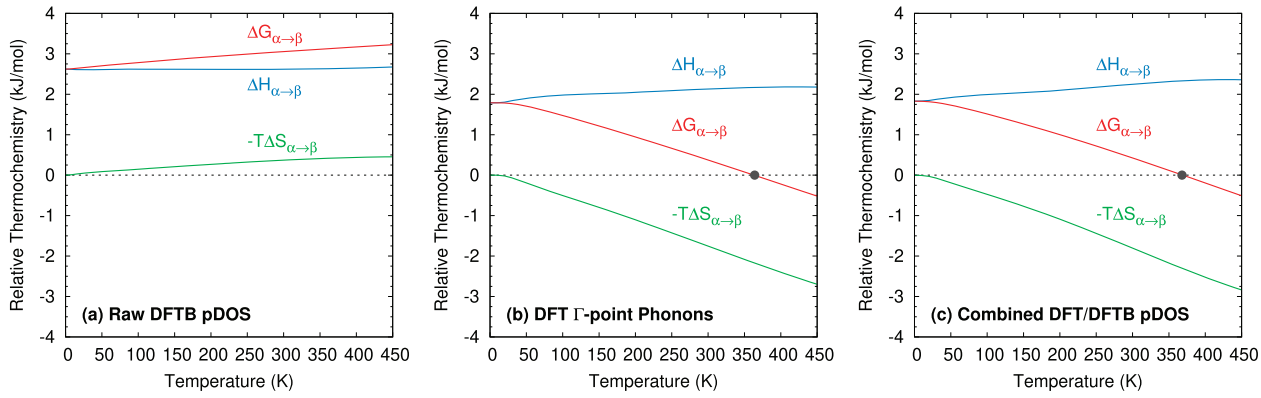

FIG. 8. Relative enthalpy, entropy ($-T\Delta S$), and Gibbs free energy differences for the $\alpha \to \beta$ phase change (in kJ/mol) using (a) the raw DFTB3-D3(BJ) phonon density of states, (b) Γ-point DFT phonons, or (c) the phonon density of states obtained after performing the B86bPBE-XDM Γ-point shift and acoustic mode corrections to the DFTB phonons. The gray points in (b) and (c) indicate the phase transition temperature.

such that the β phase is increasingly favored at higher temperatures. At 368 K, the corrected entropy becomes sufficiently large to overcome the enthalpy difference between the two phases, and the β polymorph becomes the stable phase. In other words, entropy drives the temperature-dependent phase transition, and correcting the DFTB3-D3(BJ) phonon DOS with the DFT Γ-point shift is essential to obtaining the proper enantiotropic relationship between the two phases.

For completeness, we also examine the performance of B86bPBE-XDM employing only Γ-point phonons, omitting the DFTB phonon dispersion contribution. At room temperature, the total Gibbs' free energy of each phase is ~3.5–3.75 kJ/mol smaller in magnitude without phonon dispersion. Because phonon dispersion is most pronounced in the low-frequency and acoustic modes, the majority of this difference stems from the decreased entropy in the Γ-point-only model. Nevertheless, much of this difference cancels when computing the thermochemical energy differences between the two polymorphs. As shown in Figs. 8(b) and 8(c), the enthalpy, entropy, and free energy changes differ only by a few tenths of a kJ/mol or less. Moreover, as shown in Table II, the predicted $\Delta H_{\alpha\to\beta}$ and $\Delta S_{\alpha\to\beta}$ values agree marginally better with the experiment, but the predicted phase transition temperature under ambient pressure is nearly identical (364 K vs 368 K with phonon dispersion). The strong similarity between the models with and without phonon dispersion here likely reflects the similarity of the crystal packing between the two forms.

For further evidence of the fortuitous nature of the agreement in the thermochemical properties, Fig. 9 compares the simulated inelastic neutron scattering (INS) spectra against the experimental ones from Ref. 73 for the three different phonon DOS models: raw DFTB, DFT Γ-point, and the mixed DFT/DFTB approach. For the ~50–300 cm^{-1} region where phonon dispersion is generally more appreciable, the combined DFT/DFTB phonon DOS model gives improved agreement with the experimental spectra compared to the DFT Γ-point phonon modes only. It does appear that the DFT/DFTB phonon DOS model underestimates the acoustic mode frequencies moderately, leading to an erroneous peak below ~50 cm^{-1}. The Γ-point DFT model nominally appears more faithful to the experiment in the sub-50 cm^{-1} region by virtue of neglecting the acoustic mode contributions entirely. In the high-frequency

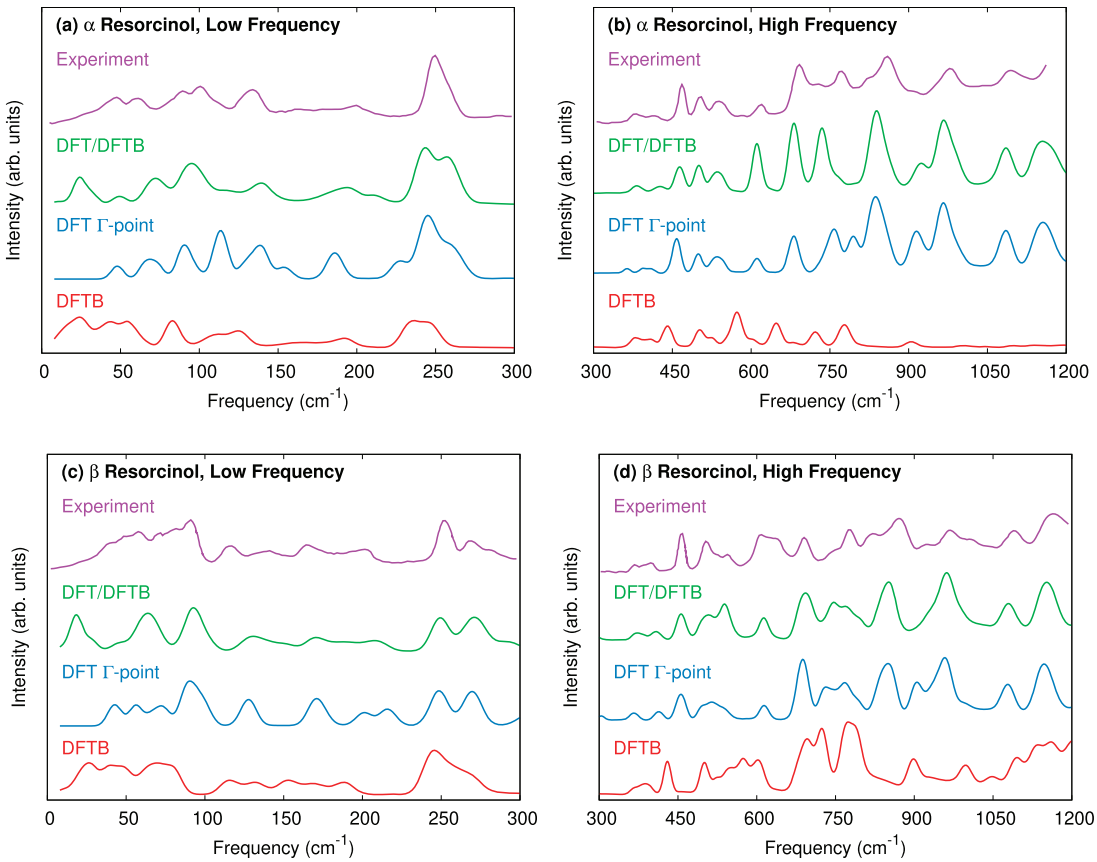

FIG. 9. Inelastic neutron scattering spectra for (a) α resorcinol in the low-frequency region, (b) α resorcinol in the high-frequency region, (c) β resorcinol in the low-frequency region, and (d) β resorcinol in the high-frequency region. The experimental spectra at 35 K are compared against the quasi-harmonic ones using the raw DFTB phonon DOS, the Γ-point DFT phonon spectra, and the combined DFT/DFTB phonon DOS.[73].

TABLE III. Comparison between experimental and predicted sublimation enthalpies at 298 K.

Method	Source	ΔH_{sub} (kJ/mol)
Expt.	Verevkin and Kozlova[121]	95.6 ± 0.6
Expt.	Gonçalves *et al.*[123]	99.7 ± 0.4
B86bPBE-XDM	This work	102.7

region above 300 cm^{-1}, the differences between the DFT Γ-point and DFT/DFTB models are smaller. In contrast to the DFT/DFTB or DFT Γ-point spectra, the INS spectrum simulated from the raw DFTB phonon DOS exhibits poor agreement with the experiment, further demonstrating the need for correcting the DFTB phonon frequencies as is done here.

Finally, we compare the predicted and experimental enthalpies of sublimation for α-resorcinol. Many experimental values for the α-resorcinol sublimation enthalpy have been reported.[117–120,122,121,123] Table III lists the averaged 298 K value of 95.6 ± 0.6 kJ/mol obtained by critical analysis of several studies[121] along with the more recent measurement by Gonçalves *et al.* of 99.7 ± 0.4 kJ/mol.[123] The theoretical sublimation enthalpy was computed for using the standard ideal gas, rigid rotor, and harmonic oscillator partition function expressions for the gas-phase species (see Ref. 110 for details). The room-temperature prediction of 102.7 kJ/mol overestimates the experimental values by 3–7 kJ/mol, depending on which experimental value is used. This error is consistent with earlier quasi-harmonic ΔH_{sub} benchmarks in small-molecule crystals[86] and DFT lattice energy benchmarks.[61,82,108] On the other hand, this error is several times larger than the error in $\Delta H_{\alpha\rightarrow\beta}$ in Table II, highlighting once again the importance of error cancellation in predicting the phase boundaries correctly. Errors in describing the intermolecular interactions in the crystalline phase are fully exposed when computing the lattice energy or sublimation enthalpy, but they cancel somewhat when examining energy differences between polymorphs.

V. CONCLUSIONS

Predicting phase boundaries between crystal polymorphs represents one of the challenging problems in modeling the organic solid state due to the extreme sensitivity of the results to small errors in the models. This challenge is compounded by the computational expense associated with computing accurate electronic energies and well-converged phonon densities of state over a range of temperatures and pressures in order to obtain the Gibbs free energies. The present work shows how DFT and DFTB can be combined in a quasi-harmonic model that accurately describes the crystal structures, thermochemistry, and phase boundaries for the α and β phases of resorcinol. The key approximation here lies in using DFT Γ-point phonon frequencies to shift the DFTB phonon density of states. Overall, the model reproduces experimental crystal structures to within 1%–2% or better, especially at lower pressures. It predicts the $\alpha \rightarrow \beta$ phase transition boundary to within a few degrees Kelvin. However, the phase transition temperature is shown to be very sensitive to small changes in the relative free energy. The level of quantitative agreement in the transition temperature reflects fortuitous error cancellation between the enthalpy and entropy, both of which are overestimated by the model relative to the experiment.

The mixture of DFT and DFTB used to compute the phonon density of states here reduces the computational costs associated by orders of magnitude,[62] making it much more feasible to model the finite-temperature thermochemistry of chemically interesting organic crystals without consuming exorbitant amounts of computer resources. At the same time, DFTB3-D3(BJ) alone proved inadequate, and the DFT-derived correction to the DFTB phonon density of states was essential in capturing the correct phase behavior in resorcinol. Therefore, the combined DFT/DFTB approach appears to provide a good balance between the computational cost and accuracy. In this particular case, Γ-point DFT phonons perform about the same as the mixed approach, although one would expect greater differences in polymorphs where the crystal packing exhibits greater differences in conformation and/or intermolecular packing.

In the future, it will be interesting to apply these same modeling procedures to crystals of more complex species, such as small-molecule pharmaceuticals. The resorcinol polymorphs here involve both hydrogen bonding and significant van der Waals dispersion interactions through the π system. In that regard, this system is reasonably representative of many rigid-molecule organic crystals. On the other hand, the similar crystal packings between the two polymorphs studied here may facilitate error cancellation to a greater extent compared to other polymorphic systems. This system also lacks the greater conformational flexibility of many larger molecules and pharmaceuticals that might complicate quasi-harmonic treatments (although some recent research has suggested that limitations of the quasi-harmonic approximation may not be well-correlated with conformational flexibility[37]).

To improve the accuracy of these approaches, it may be useful to improve the quality of the DFT electronic energies via the use of hybrid or other higher-quality density functionals,[8] inclusion of conformational energy corrections when needed,[25] or perhaps even employing post-DFT treatments where feasible.[86,124] Fortunately, the Γ-point "reference" frequencies used in the matching procedure are not restricted to DFT-GGA. This provides a particular advantage over the density functional perturbation treatment, where the implementation of hybrid density functionals is less straightforward.[125] Incorporation of additional phonon mode anharmonicity[38] might also help improve the predicted thermochemistry, especially for molecules with greater intramolecular conformational flexibility. Regardless of the specific modeling choices made, one should take care to understand how uncertainties in the computational models manifest in the final predictions and remain cognizant of the role of error cancellation in making useful thermochemical predictions for the organic solid state.[126]

AUTHORS' CONTRIBUTIONS

C. Cook and J. L. McKinley contributed equally to this work.

ACKNOWLEDGMENTS

The authors gratefully acknowledge the funding from the National Science Foundation (Grant No. CHE-1955554 to G.J.O.B.), the Graduate Research Fellowship (Grant No. 1326120 to J.L.M.), and supercomputer time from XSEDE (Grant Nos. TG-CHE110064

to G.J.O.B. and TG-CHE170098 to J.L.M.). Additional computational resources were provided by the UC Riverside high-performance computing center, which was funded by the grants from the National Science Foundation (Grant No. MRI-1429826) and the National Institutes of Health (Grant No. 1S10OD016290-01A1). We thank Dr. Ctirad Červinka for helpful discussions.

There are no conflicts of interest to declare.

DATA AVAILABILITY

The data that support the findings of this study are available from the corresponding author upon reasonable request.

REFERENCES

[1]G. M. Day, T. G. Cooper, A. J. Cruz-Cabeza, K. E. Hejczyk, H. L. Ammon, S. X. M. Boerrigter, J. S. Tan, R. G. Della Valle, E. Venuti, J. Jose, S. R. Gadre, G. R. Desiraju, T. S. Thakur, B. P. van Eijck, J. C. Facelli, V. E. Bazterra, M. B. Ferraro, D. W. M. Hofmann, M. A. Neumann, F. J. J. Leusen, J. Kendrick, S. L. Price, A. J. Misquitta, P. G. Karamertzanis, G. W. A. Welch, H. A. Scheraga, Y. A. Arnautova, M. U. Schmidt, J. van de Streek, A. K. Wolf, and B. Schweizer, "Significant progress in predicting the crystal structures of small organic molecules—A report on the fourth blind test," Acta Crystallogr., Sect. B **65**, 107–125 (2009).

[2]M. A. Neumann, F. J. J. Leusen, and J. Kendrick, "A major advance in crystal structure prediction," Angew. Chem., Int. Ed. **47**, 2427–2430 (2008).

[3]D. A. Bardwell, C. S. Adjiman, Y. A. Arnautova, E. Bartashevich, S. X. M. Boerrigter, D. E. Braun, A. J. Cruz-Cabeza, G. M. Day, R. G. Della Valle, G. R. Desiraju, B. P. van Eijck, J. C. Facelli, M. B. Ferraro, D. Grillo, M. Habgood, D. W. M. Hofmann, F. Hofmann, K. V. J. Jose, P. G. Karamertzanis, A. V. Kazantsev, J. Kendrick, L. N. Kuleshova, F. J. J. Leusen, A. V. Maleev, A. J. Misquitta, S. Mohamed, R. J. Needs, M. A. Neumann, D. Nikylov, A. M. Orendt, R. Pal, C. C. Pantelides, C. J. Pickard, L. S. Price, S. L. Price, H. A. Scheraga, J. van de Streek, T. S. Thakur, S. Tiwari, E. Venuti, and I. K. Zhitkov, "Towards crystal structure prediction of complex organic compounds—A report on the fifth blind test," Acta Crystallogr., Sect. B **67**, 535–551 (2011).

[4]A. M. Reilly, R. I. Cooper, C. S. Adjiman, S. Bhattacharya, A. D. Boese, J. G. Brandenburg, P. J. Bygrave, R. Bylsma, J. E. Campbell, R. Car, D. H. Case, R. Chadha, J. C. Cole, K. Cosburn, H. M. Cuppen, F. Curtis, G. M. Day, R. A. DiStasio, Jr., A. Dzyabchenko, B. P. van Eijck, D. M. Elking, J. A. van den Ende, J. C. Facelli, M. B. Ferraro, L. Fusti-Molnar, C.-A. Gatsiou, T. S. Gee, R. de Gelder, L. M. Ghiringhelli, H. Goto, S. Grimme, R. Guo, D. W. M. Hofmann, J. Hoja, R. K. Hylton, L. Iuzzolino, W. Jankiewicz, D. T. de Jong, J. Kendrick, N. J. J. de Klerk, H.-Y. Ko, L. N. Kuleshova, X. Li, S. Lohani, F. J. J. Leusen, A. M. Lund, J. Lv, Y. Ma, N. Marom, A. E. Masunov, P. McCabe, D. P. McMahon, H. Meekes, M. P. Metz, A. J. Misquitta, S. Mohamed, B. Monserrat, R. J. Needs, M. A. Neumann, J. Nyman, S. Obata, H. Oberhofer, A. R. Oganov, A. M. Orendt, G. I. Pagola, C. C. Pantelides, C. J. Pickard, R. Podeszwa, L. S. Price, S. L. Price, A. Pulido, M. G. Read, K. Reuter, E. Schneider, C. Schober, G. P. Shields, P. Singh, I. J. Sugden, K. Szalewicz, C. R. Taylor, A. Tkatchenko, M. E. Tuckerman, F. Vacarro, M. Vasileiadis, A. Vazquez-Mayagoitia, L. Vogt, Y. Wang, R. E. Watson, G. A. de Wijs, J. Yang, Q. Zhu, and C. R. Groom, "Report on the sixth blind test of organic crystal structure prediction methods," Acta Crystallogr., Sect. B **72**, 439–459 (2016).

[5]A. Asmadi, M. A. Neumann, J. Kendrick, P. Girard, M.-A. Perrin, and F. J. J. Leusen, "Revisiting the blind tests in crystal structure prediction: Accurate energy ranking of molecular crystals," J. Phys. Chem. B **113**, 16303–16313 (2009).

[6]S. R. Whittleton, A. Otero-de-la-Roza, and E. R. Johnson, "Exchange-hole dipole dispersion model for accurate energy ranking in molecular crystal structure prediction," J. Chem. Theory Comput. **13**, 441–450 (2017).

[7]S. R. Whittleton, A. Otero-de-la-Roza, and E. R. Johnson, "Exchange-hole dipole dispersion model for accurate energy ranking in molecular crystal structure prediction II: Nonplanar molecules," J. Chem. Theory Comput. **13**, 5332–5342 (2017).

[8]J. Hoja, H.-Y. Ko, M. A. Neumann, R. Car, R. A. DiStasio, and A. Tkatchenko, "Reliable and practical computational description of molecular crystal polymorphs," Sci. Adv. **5**, eaau3338 (2019).

[9]S. L. Price and S. M. Reutzel-Edens, "The potential of computed crystal energy landscapes to aid solid-form development," Drug Discovery Today **21**, 912–923 (2016).

[10]S. L. Price, D. E. Braun, and S. M. Reutzel-Edens, "Can computed crystal energy landscapes help understand pharmaceutical solids?," Chem. Commun. **52**, 7065–7077 (2016).

[11]D. E. Braun, J. A. McMahon, L. H. Koztecki, S. L. Price, and S. M. Reutzel-Edens, "Contrasting polymorphism of related small molecule drugs correlated and guided by the computed crystal energy landscape," Cryst. Growth Des. **14**, 2056–2072 (2014).

[12]M. A. Neumann, J. van de Streek, F. P. A. Fabbiani, P. Hidber, and O. Grassmann, "Combined crystal structure prediction and high-pressure crystallization in rational pharmaceutical polymorph screening," Nat. Commun. **6**, 7793 (2015).

[13]D. E. Braun, S. R. Lingireddy, M. D. Beidelschies, R. Guo, P. Müller, S. L. Price, and S. M. Reutzel-Edens, "Unraveling complexity in the solid form screening of a pharmaceutical salt: Why so many forms? Why so few?," Cryst. Growth Des. **17**, 5349–5365 (2017).

[14]G. R. Woollam, M. A. Neumann, T. Wagner, and R. J. Davey, "The importance of configurational disorder in crystal structure prediction: The case of loratadine," Faraday Discuss. **211**, 209–234 (2018).

[15]R. M. Bhardwaj, J. A. McMahon, J. Nyman, L. S. Price, S. Konar, I. D. H. Oswald, C. R. Pulham, S. L. Price, and S. M. Reutzel-Edens, "A prolific solvate former, galunisertib, under the pressure of crystal structure prediction, produces ten diverse polymorphs," J. Am. Chem. Soc. **141**, 13887–13897 (2019).

[16]M. Mortazavi, J. Hoja, L. Aerts, L. Quéré, J. van de Streek, M. A. Neumann, and A. Tkatchenko, "Computational polymorph screening reveals late-appearing and poorly-soluble form of rotigotine," Commun. Chem. **2**, 70 (2019).

[17]S. Askin, J. K. Cockcroft, L. S. Price, A. D. Gonçalves, M. Zhao, D. A. Tocher, G. R. Williams, S. Gaisford, and D. Q. M. Craig, "Olanzapine form IV: Discovery of a new polymorphic form enabled by computed crystal energy landscapes," Cryst. Growth Des. **19**, 2751–2757 (2019).

[18]S. L. Price, "Why don't we find more polymorphs?," Acta Crystallogr., Sect. B **69**, 313–328 (2013).

[19]W. C. McCrone, in *Physics and Chemistry of the Organic Solid State*, edited by D. Fox, M. M. Labes, and A. Weissberger (Wiley-Interscience, New York, 1965), Vol. 2, pp. 725–767.

[20]M. Vasileiadis, A. V. Kazantsev, P. G. Karamertzanis, C. S. Adjiman, and C. C. Pantelides, "The polymorphs of ROY: Application of a systematic crystal structure prediction technique," Acta Crystallogr., Sect. B **68**, 677–685 (2012).

[21]J. Nyman, L. Yu, and S. M. Reutzel-Edens, "Accuracy and reproducibility in crystal structure prediction: The curious case of ROY," CrystEngComm **21**, 2080–2088 (2019).

[22]M. Vasileiadis, C. C. Pantelides, and C. S. Adjiman, "Prediction of the crystal structures of axitinib, a polymorphic pharmaceutical molecule," Chem. Eng. Sci. **121**, 60–76 (2015).

[23]A. R. Tyler, R. Ragbirsingh, C. J. McMonagle, P. G. Waddell, S. E. Heaps, J. W. Steed, P. Thaw, M. J. Hall, and M. R. Probert, "Encapsulated nanodroplet crystallization of organic-soluble small molecules," Chem **6**, 1755–1765 (2020).

[24]X. Li, X. Ou, H. Rong, S. Huang, J. Nyman, L. Yu, and M. Lu, "The twelfth solved structure of ROY: Single crystals of Y04 grown from melt microdroplets," Cryst. Growth Des. **20**, 7093–7097 (2020).

[25]C. Greenwell and G. J. O. Beran, "Inaccurate conformational energies still hinder crystal structure prediction in flexible organic molecules," Cryst. Growth Des. **20**, 4875–4881 (2020).

[26]S. L. Price, "Is zeroth order crystal structure prediction (CSP_0) coming to maturity? What should we aim for in an ideal crystal structure prediction code?," Faraday Discuss. **211**, 9–30 (2018).

[27]P. Raiteri, R. Martoňák, and M. Parrinello, "Exploring polymorphism: The case of benzene," Angew. Chem., Int. Ed. **44**, 3769–3773 (2005).

[28]E. C. Dybeck, D. P. McMahon, G. M. Day, and M. R. Shirts, "Exploring the multi-minima behavior of small molecule crystal polymorphs at finite temperature," Cryst. Growth Des. **19**, 5568–5580 (2019).

[29]N. F. Francia, L. S. Price, J. Nyman, S. L. Price, and M. Salvalaglio, "Systematic finite-temperature reduction of crystal energy landscapes," Cryst. Growth Des. **20**, 6847–6862 (2020).

[30]N. L. Allan, G. D. Barrera, T. H. K. Barron, and M. B. Taylor, "Evaluation of thermodynamic properties of solids by quasiharmonic lattice dynamics," Int. J. Thermophys. **22**, 535–546 (2001).
[31]R. P. Stoffel, C. Wessel, M.-W. Lumey, and R. Dronskowski, "*Ab initio* thermochemistry of solid-state materials," Angew. Chem., Int. Ed. **49**, 5242–5266 (2010).
[32]C. Červinka, M. Fulem, R. P. Stoffel, and R. Dronskowski, "Thermodynamic properties of molecular crystals calculated within the quasi-harmonic approximation," J. Phys. Chem. A **120**, 2022–2034 (2016).
[33]C. Červinka and G. J. O. Beran, "*Ab initio* prediction of the polymorph phase diagram for crystalline methanol," Chem. Sci. **9**, 4622–4629 (2018).
[34]N. P. Schieber, E. C. Dybeck, and M. R. Shirts, "Using reweighting and free energy surface interpolation to predict solid-solid phase diagrams," J. Chem. Phys. **148**, 144104 (2018).
[35]E. C. Dybeck, N. S. Abraham, N. P. Schieber, and M. R. Shirts, "Capturing entropic contributions to temperature-mediated polymorphic transformations through molecular modeling," Cryst. Growth Des. **17**, 1775–1787 (2017).
[36]N. S. Abraham and M. R. Shirts, "Thermal gradient approach for the quasiharmonic approximation and its application to improved treatment of anisotropic expansion," J. Chem. Theory Comput. **14**, 5904–5919 (2018).
[37]N. S. Abraham and M. R. Shirts, "Adding anisotropy to the standard quasiharmonic approximation still fails in several ways to capture organic crystal thermodynamics," Cryst. Growth Des. **19**, 6911–6924 (2019).
[38]J. Hoja and A. Tkatchenko, "First-principles stability ranking of molecular crystal polymorphs with the DFT+MBD approach," Faraday Discuss. **211**, 253–274 (2018).
[39]T.-Q. Yu and M. Tuckerman, "Temperature-accelerated method for exploring polymorphism in molecular crystals based on free energy," Phys. Rev. Lett. **107**, 015701 (2011).
[40]E. Schneider, L. Vogt, and M. E. Tuckerman, "Exploring polymorphism of benzene and naphthalene with free energy based enhanced molecular dynamics," Acta Crystallogr., Sect. B **72**, 542–550 (2016).
[41]M. Rossi, P. Gasparotto, and M. Ceriotti, "Anharmonic and quantum fluctuations in molecular crystals: A first-principles study of the stability of paracetamol," Phys. Rev. Lett. **117**, 115702 (2016).
[42]N. Raimbault, V. Athavale, and M. Rossi, "Anharmonic effects in the low-frequency vibrational modes of aspirin and paracetamol crystals," Phys. Rev. Mater. **3**, 053605 (2019).
[43]H. Y. Ko, R. A. Distasio, B. Santra, and R. Car, "Thermal expansion in dispersion-bound molecular crystals," Phys. Rev. Mater. **2**, 055603 (2018).
[44]B. Cheng, E. A. Engel, J. Behler, C. Dellago, and M. Ceriotti, "*Ab initio* thermodynamics of liquid and solid water," Proc. Natl. Acad. Sci. U. S. A. **116**, 1110–1115 (2019).
[45]Y. Abramov, G. Sun, Y. Zhou, M. Yang, Q. Zeng, and Z. Shen, "Solid-form transition temperature prediction from a virtual polymorph screening: A reality check," Cryst. Growth Des. **19**, 7132–7137 (2019).
[46]S. A. Bonev, F. Gygi, T. Ogitsu, and G. Galli, "High-pressure molecular phases of solid carbon dioxide," Phys. Rev. Lett. **91**, 065501 (2003).
[47]J. Li, O. Sode, G. A. Voth, and S. Hirata, "A solid-solid phase transition in carbon dioxide at high pressures and intermediate temperatures," Nat. Commun. **4**, 2647 (2013).
[48]Y. Han, J. Liu, L. Huang, X. He, and J. Li, "Predicting the phase diagram of solid carbon dioxide at high pressure from first principles," npj Quantum Mater. **4**, 10 (2019).
[49]Y. Han, J. Liu, and J. Li, "Molecular structure determination of solid carbon dioxide phase IV at high pressures and temperatures based on Møller-Plesset perturbation theory," Int. J. Quantum Chem. **120**, e26397 (2020).
[50]L. Huang, Y. Han, X. He, and J. Li, "*Ab initio*-enabled phase transition prediction of solid carbon dioxide at ultra-high temperatures," RSC Adv. **10**, 236–243 (2020).
[51]Y. Han, Z. Wang, and J. Li, "Neural networks accelerate the *ab initio* prediction of solid–solid phase transitions at high pressures," J. Phys. Chem. Lett. **12**, 132–137 (2021).
[52]Q. Lu, I. Ali, and J. Li, "Prediction of properties from first principles with quantitative accuracy: Six representative ice phases," New J. Chem. **44**, 21012–21020 (2020).
[53]J. Xu, J. Liu, J. Liu, W. Hu, X. He, and J. Li, "Phase transition of ice at high pressures and low temperatures," Molecules **25**, 486 (2020).
[54]J. Kotakoski and K. Albe, "First-principles calculations on solid nitrogen: A comparative study of high-pressure phases," Phys. Rev. B **77**, 144109 (2008).
[55]C. J. Pickard and R. J. Needs, "High-pressure phases of nitrogen," Phys. Rev. Lett. **102**, 125702 (2009).
[56]A. Erba, L. Maschio, C. Pisani, and S. Casassa, "Pressure-induced transitions in solid nitrogen: Role of dispersive interactions," Phys. Rev. B **84**, 012101 (2011).
[57]A. Erba, L. Maschio, S. Salustro, and S. Casassa, "A post-Hartree–Fock study of pressure-induced phase transitions in solid nitrogen: The case of the α, γ, and ϵ low-pressure phases," J. Chem. Phys. **134**, 074502 (2011).
[58]D. Plašienka and R. Martoňák, "Transformation pathways in high-pressure solid nitrogen: From molecular N_2 to polymeric cg-N," J. Chem. Phys. **142**, 094505 (2015).
[59]W. Sontising and G. J. O. Beran, "Theoretical assessment of the structure and stability of the λ phase of nitrogen," Phys. Rev. Mater. **3**, 095002 (2019).
[60]X.-D. Wen, R. Hoffmann, and N. W. Ashcroft, "Benzene under high pressure: A story of molecular crystals transforming to saturated networks, with a possible intermediate metallic phase," J. Am. Chem. Soc. **133**, 9023–9035 (2011).
[61]G. J. O. Beran, "Modeling polymorphic molecular crystals with electronic structure theory," Chem. Rev. **116**, 5567–5613 (2016).
[62]C. Cook and G. J. O. Beran, "Reduced-cost supercell approach for computing accurate phonon density of states in organic crystals," J. Chem. Phys. **153**, 224105 (2020).
[63]J. G. Brandenburg and S. Grimme, "Accurate modeling of organic molecular crystals by dispersion-corrected density functional tight binding (DFTB)," J. Phys. Chem. Lett. **5**, 1785–1789 (2014).
[64]J. G. Brandenburg, T. Maas, and S. Grimme, "Benchmarking DFT and semiempirical methods on structures and lattice energies for ten ice polymorphs," J. Chem. Phys. **142**, 124104 (2015).
[65]H. K. Buchholz, R. K. Hylton, J. G. Brandenburg, A. Seidel-Morgenstern, H. Lorenz, M. Stein, and S. L. Price, "Thermochemistry of racemic and enantiopure organic crystals for predicting enantiomer separation," Cryst. Growth Des. **17**, 4676–4686 (2017).
[66]G. A. Dolgonos, O. A. Loboda, and A. D. Boese, "Development of embedded and performance of density functional methods for molecular crystals," J. Phys. Chem. A **122**, 708–713 (2018).
[67]L. Iuzzolino, P. McCabe, S. L. Price, and J. G. Brandenburg, "Crystal structure prediction of flexible pharmaceutical-like molecules: Density functional tight-binding as an intermediate optimisation method and for free energy estimation," Faraday Discuss. **211**, 275–296 (2018).
[68]M. Mortazavi, J. G. Brandenburg, R. J. Maurer, and A. Tkatchenko, "Structure and stability of molecular crystals with many-body dispersion-inclusive density functional tight binding," J. Phys. Chem. Lett. **9**, 399–405 (2018).
[69]J. G. Brandenburg, J. Potticary, H. A. Sparkes, S. L. Price, and S. R. Hall, "Thermal expansion of carbamazepine: Systematic crystallographic measurements challenge quantum chemical calculations," J. Phys. Chem. Lett. **8**, 4319–4324 (2017).
[70]F. Safari, A. Olejniczak, and A. Katrusiak, "Pressure-dependent crystallization preference of resorcinol polymorphs," Cryst. Growth Des. **19**, 5629–5635 (2019).
[71]E. H. Lee, "A practical guide to pharmaceutical polymorph screening & selection," Asian J. Pharm. Sci. **9**, 163–175 (2014).
[72]S. E. Kichanov, D. P. Kozlenko, P. Bilski, J. Wąsicki, W. Nawrocik, A. Medek, B. C. Hancock, E. V. Lukin, C. Lathe, L. S. Dubrovinsky, and B. N. Savenko, "The polymorphic phase transformations in resorcinol at high pressure," J. Mol. Struct. **1006**, 337–343 (2011).
[73]K. Drużbicki, E. Mikuli, N. Pałka, S. Zalewski, and M. D. Ossowska-Chruściel, "Polymorphism of resorcinol explored by complementary vibrational spectroscopy (FT-RS, THz-TDS, INS) and first-principles solid-state computations (Plane-Wave DFT)," J. Phys. Chem. B **119**, 1681–1695 (2015).
[74]Y. Ebisuzaki, L. H. Askari, A. M. Bryan, and M. F. Nicol, "Phase transitions in resorcinal," J. Chem. Phys. **87**, 6659–6664 (1987).

[75]S. K. Deb, M. A. Rekha, A. P. Roy, V. Vijayakumar, S. Meenakshi, and B. K. Godwal, "Raman-scattering study of high-pressure phase transition and amorphization of resorcinol," Phys. Rev. B **47**, 11491–11494 (1993).
[76]R. Rao, T. Sakuntala, and B. K. Godwal, "Evidence for high-pressure polymorphism in resorcinol," Phys. Rev. B **65**, 054108 (2002).
[77]Q. Zhu, A. G. Shtukenberg, D. J. Carter, T.-Q. Yu, J. Yang, M. Chen, P. Raiteri, A. R. Oganov, B. Pokroy, I. Polishchuk, P. J. Bygrave, G. M. Day, A. L. Rohl, M. E. Tuckerman, and B. Kahr, "Resorcinol crystallization from the melt: A new ambient phase and new "riddles"," J. Am. Chem. Soc. **138**, 4881–4889 (2016).
[78]M. T. Dove, "Introduction to the theory of lattice dynamics," Collection SFN **12**, 123–159 (2011).
[79]D. Alfè, "PHON: A program to calculate phonons using the small displacement method," Comput. Phys. Commun. **180**, 2622–2633 (2009).
[80]A. Togo and I. Tanaka, "First principles phonon calculations in materials science," Scr. Mater. **108**, 1–5 (2015).
[81]S. Baroni, S. de Gironcoli, A. Dal Corso, and P. Giannozzi, "Phonons and related crystal properties from density functional perturbation theory," Rev. Mod. Phys. **73**, 515–562 (2001).
[82]A. M. Reilly and A. Tkatchenko, "Understanding the role of vibrations, exact exchange, and many-body van der Waals interactions in the cohesive properties of molecular crystals," J. Chem. Phys. **139**, 024705 (2013).
[83]A. Erba, "On combining temperature and pressure effects on structural properties of crystals with standard *ab initio* techniques," J. Chem. Phys. **141**, 124115 (2014).
[84]J. Nyman, O. S. Pundyke, and G. M. Day, "Accurate force fields and methods for modelling organic molecular crystals at finite temperatures," Phys. Chem. Chem. Phys. **18**, 15828–15837 (2016).
[85]C. Červinka and G. J. O. Beran, "*Ab initio* thermodynamic properties and their uncertainties for crystalline α-methanol," Phys. Chem. Chem. Phys. **19**, 29940–29953 (2017).
[86]J. L. McKinley and G. J. O. Beran, "Identifying pragmatic quasi-harmonic electronic structure approaches for modeling molecular crystal thermal expansion," Faraday Discuss. **211**, 181–207 (2018).
[87]C. Červinka and G. J. O. Beran, "Towards reliable *ab initio* sublimation pressures for organic molecular crystals—Are we there yet?," Phys. Chem. Chem. Phys. **21**, 14799–14810 (2019).
[88]J. L. McKinley and G. J. O. Beran, "Improving predicted nuclear magnetic resonance chemical shifts using the quasi-harmonic approximation," J. Chem. Theory Comput. **15**, 5259–5274 (2019).
[89]F. D. Murnaghan, "The compressibility of media under extreme pressures," Proc. Natl. Acad. Sci. U. S. A. **30**, 244–247 (1944).
[90]A. Erba, J. Maul, and B. Civalleri, "Thermal properties of molecular crystals through dispersion-corrected quasi-harmonic *ab initio* calculations: The case of urea," Chem. Commun. **52**, 1820–1823 (2016).
[91]C. Červinka and M. Fulem, "State-of-The-Art calculations of sublimation enthalpies for selected molecular crystals and their computational uncertainty," J. Chem. Theory Comput. **13**, 2840–2850 (2017).
[92]J. Hoja, A. M. Reilly, and A. Tkatchenko, "First-principles modeling of molecular crystals: Structures and stabilities, temperature and pressure," Wiley Interdiscip. Rev.: Comput. Mol. Sci. **7**, e1294 (2017).
[93]L. Monacelli, I. Errea, M. Calandra, and F. Mauri, "Pressure and stress tensor of complex anharmonic crystals within the stochastic self-consistent harmonic approximation," Phys. Rev. B **98**, 024106 (2018).
[94]F. R. Fronczek, CCDC 168981: Experimental Crystal Structure Determination, 2001.
[95]G. E. Bacon and E. J. Lisher, "A neutron powder diffraction study of deuterated α- and β-resorcinol," Acta Crystallogr., Sect. B **36**, 1908–1916 (1980).
[96]P. Giannozzi, O. Andreussi, T. Brumme, O. Bunau, M. Buongiorno Nardelli, M. Calandra, R. Car, C. Cavazzoni, D. Ceresoli, M. Cococcioni, N. Colonna, I. Carnimeo, A. Dal Corso, S. de Gironcoli, P. Delugas, R. A. DiStasio, A. Ferretti, A. Floris, G. Fratesi, G. Fugallo, R. Gebauer, U. Gerstmann, F. Giustino, T. Gorni, J. Jia, M. Kawamura, H.-Y. Ko, A. Kokalj, E. Küçükbenli, M. Lazzeri, M. Marsili, N. Marzari, F. Mauri, N. L. Nguyen, H.-V. Nguyen, A. Otero-de-la-Roza, L. Paulatto, S. Poncé, D. Rocca, R. Sabatini, B. Santra, M. Schlipf, A. P. Seitsonen, A. Smogunov, I. Timrov, T. Thonhauser, P. Umari, N. Vast, X. Wu, and S. Baroni, "Advanced capabilities for materials modelling with quantum ESPRESSO," J. Phys.: Condens. Matter **29**, 465901 (2017).
[97]A. D. Becke, "On the large-gradient behavior of the density functional exchange energy," J. Chem. Phys. **85**, 7184–7187 (1986).
[98]J. P. Perdew, K. Burke, and M. Ernzerhof, "Generalized gradient approximation made simple," Phys. Rev. Lett. **77**, 3865 (1996).
[99]A. Otero-de-la-Roza and E. R. Johnson, "van der Waals interactions in solids using the exchange-hole dipole moment model," J. Chem. Phys. **136**, 174109 (2012).
[100]A. Otero-De-La-Roza, B. H. Cao, I. K. Price, J. E. Hein, and E. R. Johnson, "Predicting the relative solubilities of racemic and enantiopure crystals by density-functional theory," Angew. Chem., Int. Ed. **53**, 7879–7882 (2014).
[101]P. Giannozzi, S. Baroni, N. Bonini, M. Calandra, R. Car, C. Cavazzoni, D. Ceresoli, G. L. Chiarotti, M. Cococcioni, I. Dabo, A. Dal Corso, S. de Gironcoli, S. Fabris, G. Fratesi, R. Gebauer, U. Gerstmann, C. Gougoussis, A. Kokalj, M. Lazzeri, L. Martin-Samos, N. Marzari, F. Mauri, R. Mazzarello, S. Paolini, A. Pasquarello, L. Paulatto, C. Sbraccia, S. Scandolo, G. Sclauzero, A. P. Seitsonen, A. Smogunov, P. Umari, and R. M. Wentzcovitch, "Quantum ESPRESSO: A modular and open-source software project for quantum simulations of materials," J. Phys.: Condens. Matter **21**, 395502 (2009).
[102]H. J. Monkhorst and J. D. Pack, "Special points for Brillouin-zone integrations," Phys. Rev. B **13**, 5188–5192 (1976).
[103]B. Aradi, B. Hourahine, and T. Frauenheim, "DFTB+, a sparse matrix-based implementation of the DFTB method," J. Phys. Chem. A **111**, 5678–5684 (2007).
[104]B. Hourahine, B. Aradi, V. Blum, F. Bonafé, A. Buccheri, C. Camacho, C. Cevallos, M. Y. Deshaye, T. Dumitrică, A. Dominguez, S. Ehlert, M. Elstner, T. van der Heide, J. Hermann, S. Irle, J. J. Kranz, C. Köhler, T. Kowalczyk, T. Kubař, I. S. Lee, V. Lutsker, R. J. Maurer, S. K. Min, I. Mitchell, C. Negre, T. A. Niehaus, A. M. N. Niklasson, A. J. Page, A. Pecchia, G. Penazzi, M. P. Persson, J. Řezáč, C. G. Sánchez, M. Sternberg, M. Stöhr, F. Stuckenberg, A. Tkatchenko, V. W. Yu, and T. Frauenheim, "DFTB+, a software package for efficient approximate density functional theory based atomistic simulations," J. Chem. Phys. **152**, 124101 (2020).
[105]M. Gaus, A. Goez, and M. Elstner, "Parametrization and benchmark of DFTB3 for organic molecules," J. Chem. Theory Comput. **9**, 338–354 (2013).
[106]A. S. Christensen, T. Kubař, Q. Cui, and M. Elstner, "Semiempirical quantum mechanical methods for noncovalent interactions for chemical and biochemical applications," Chem. Rev. **116**, 5301–5337 (2016).
[107]S. Grimme, J. Antony, S. Ehrlich, and H. Krieg, "A consistent and accurate *ab initio* parametrization of density functional dispersion correction (DFT-D) for the 94 elements H-Pu," J. Chem. Phys. **132**, 154104 (2010).
[108]A. Otero-de-la-Roza and E. R. Johnson, "A benchmark for non-covalent interactions in solids," J. Chem. Phys. **137**, 054103 (2012).
[109]Y. N. Heit, K. D. Nanda, and G. J. O. Beran, "Predicting finite-temperature properties of crystalline carbon dioxide from first principles with quantitative accuracy," Chem. Sci. **7**, 246–255 (2016).
[110]Y. N. Heit and G. J. O. Beran, "How important is thermal expansion for predicting molecular crystal structures and thermochemistry at finite temperatures?," Acta Crystallogr., Sect. B **72**, 514–529 (2016).
[111]W. Sontising, Y. N. Heit, J. L. McKinley, and G. J. O. Beran, "Theoretical predictions suggest carbon dioxide phases III and VII are identical," Chem. Sci. **8**, 7374–7382 (2017).
[112]J. George, R. Wang, U. Englert, and R. Dronskowski, "Lattice thermal expansion and anisotropic displacements in urea, bromomalonic aldehyde, pentachloropyridine, and naphthalene," J. Chem. Phys. **147**, 074112 (2017).
[113]H. Z. Lautz, "Uber die Beziehungen instabiler Formen zu stabilen," Phys. Chem. **84**, 611 (1913).
[114]J. M. Robertson and A. R. Ubbelohde, "A new form of resorcinol. II. Thermodynamic properties in relation to structure," Proc. R. Soc. London A **167**, 136–147 (1938).
[115]P. Bret-Dibat and A. Lichanot, "Proprietes thermodynamiques des isomeres de position de benzenes disubstitues en phase condensee," Thermochim. Acta **147**, 261–271 (1989).

[116]Y. Q. Cheng, L. L. Daemen, A. I. Kolesnikov, and A. J. Ramirez-Cuesta, "Simulation of inelastic neutron scattering spectra using OCLIMAX," J. Chem. Theory Comput. **15**, 1974–1982 (2019).
[117]K. L. Wolf and H. G. Trieschmann, "Über sublimationswärmen organischer moleküle," Z. Phys. Chem. B **27**, 376–380 (1934).
[118]H. Hoyer and W. Z. Peperle, "Dampfdruckmessungen an organischen Substanzen und ihre Sublimationswarmen," Electrochem. **62**, 61–66 (1958).
[119]R. Bender, V. Bieling, and G. Maurer, "The vapour pressures of solids: Anthracene, hydroquinone, and resorcinol," J. Chem. Thermodyn. **15**, 585–594 (1983).
[120]R. Sabbah and E. N. L. E. Buluku, "Étude thermodynamique des trois isomres du dihydroxybenzne," Can. J. Chem. **69**, 481–488 (1991).
[121]S. P. Verevkin and S. A. Kozlova, "Di-hydroxybenzenes: Catechol, resorcinol, and hydroquinone. Enthalpies of phase transitions revisited," Thermochim. Acta **471**, 33–42 (2008).
[122]W. Acree and J. S. Chickos, "Phase transition enthalpy measurements of organic and organometallic compounds. Sublimation, vaporization and fusion enthalpies from 1880 to 2010," J. Phys. Chem. Ref. Data **39**, 043101 (2010).
[123]E. M. Gonçalves, F. Agapito, T. S. Almeida, and J. A. Martinho Simões, "Enthalpies of formation of dihydroxybenzenes revisited: Combining experimental and high-level *ab initio* data," J. Chem. Thermodyn. **73**, 90–96 (2014).
[124]C. Greenwell, J. L. McKinley, P. Zhang, Q. Zeng, G. Sun, B. Li, S. Wen, and G. J. O. Beran, "Overcoming the difficulties of predicting conformational polymorph energetics in molecular crystals via correlated wavefunction methods," Chem. Sci. **11**, 2200–2214 (2020).
[125]J. H. Lloyd-Williams and B. Monserrat, "Lattice dynamics and electron-phonon coupling calculations using nondiagonal supercells," Phys. Rev. B **92**, 184301 (2015).
[126]I. Natkaniec, D. Chudoba, Hetmańczyk, V. Y. Kazimirov, J. Krawczyk, I. L. Sashin, and S. Zalewski, "Parameters of the NERA spectrometer for cold and thermal moderators of the IBR-2 pulsed reactor," J. Phys.: Conf. Ser. **554**, 012002 (2014).